A&A 392, 653–669 (2002)
DOI: 10.1051/0004-6361:20020941

Astronomy & Astrophysics

Stellar and wind properties of LMC WC4 stars

A metallicity dependence for Wolf-Rayet mass-loss rates⋆

P. A. Crowther[1], L. Dessart[1,2], D. J. Hillier[3], J. B. Abbott[1], and A. W. Fullerton[4,5]

[1] Department of Physics & Astronomy, UCL, Gower Street, London WC1E 6BT, UK
e-mail: jba@star.ucl.ac.uk
[2] Sterrenkundig Institut, Universiteit Utrecht, PO Box 80000, 3508 TA Utrecht, The Netherlands
e-mail: L.Dessart@astro.uu.nl
[3] Department of Physics & Astronomy, University of Pittsburgh, 3941 O'Hara Street, PA 15260, USA
e-mail: jdh@phyast.pitt.edu
[4] Dept. of Physics & Astronomy, University of Victoria, PO Box 3055, Victoria, BC, V8W 3P6, Canada
[5] Department of Physics & Astronomy, Johns Hopkins University, 3400 North Charles St., Baltimore, MD 21218, USA
e-mail: awf@pha.jhu.edu

Received 14 May 2002 / Accepted 21 June 2002

Abstract. We use ultraviolet space-based (*FUSE, HST*) and optical/IR ground-based (2.3 m MSSSO, NTT) spectroscopy to determine the physical parameters of six WC4-type Wolf-Rayet stars in the Large Magellanic Cloud. Stellar parameters are revised significantly relative to Gräfener et al. (1998) based on improved observations and more sophisticated model atmosphere codes, which account for line blanketing and clumping. We find that stellar luminosities are revised upwards by up to 0.4 dex, with surface abundances spanning a lower range of $0.1 \leq$ C/He ≤ 0.35 (20–45% carbon by mass) and O/He ≤ 0.06 ($\leq$10% oxygen by mass). Relative to Galactic WC5–8 stars at known distance, and analysed in a similar manner, LMC WC4 stars possess systematically higher stellar luminosities, ~0.2 dex lower wind densities, yet a similar range of surface chemistries. We illustrate how the classification C III λ5696 line is extremely sensitive to wind density, such that this is the principal difference between the subtype distribution of LMC and Galactic early-type WC stars. Temperature differences do play a role, but carbon abundance does not affect WC spectral types. We illustrate the effect of varying temperature and mass-loss rate on the WC spectral type for HD 32257 (WC4, LMC) and HD 156385 (WC7, Galaxy) which possess similar abundances and luminosities. Using the latest evolutionary models, pre-supernova stellar masses in the range 11–19 $M_{\odot}$ are anticipated for LMC WC4 stars, with 7–14 $M_{\odot}$ for Galactic WC stars with known distances. These values are consistent with pre-cursors of bright type-Ic supernovae such as SN 1998bw (alias GRB 980425) for which a minimum total mass of C and O of 14 $M_{\odot}$ has been independently derived.

Key words. stars: Wolf-Rayet – stars: fundamental parameters – stars: evolution – stars: abundances – galaxies: Magellanic Clouds

1. Introduction

The ultimate fate of the most massive stars is likely to be a type Ib or Ic Supernova (SN) explosion. Type Ib's, conspicuous for the absence of hydrogen in their spectra, likely correspond to WN-type Wolf-Rayet (WR) stars, whilst WC or WO stars are thought to be responsible for type Ic SN, since both hydrogen and helium are absent from their (early) spectra. Are the properties of WC stars immediately prior to their proposed SN explosion consistent with that of such SN? Models of WR stars and SN are now sufficiently advanced to facilitate such comparisons for the first time.

Over the past couple of decades, spectroscopic tools for the quantitative analysis of WR stars have advanced sufficiently (e.g. Hillier & Miller 1998) to permit the reliable determination of abundances (Herald et al. 2001), masses (De Marco et al. 2000) and ionizing fluxes (Crowther et al. 1999). Armed with these tools, we are now in an unprecedented position to investigate such stars in the Local Group and beyond (e.g. Smartt et al. 2001). Already, high quality observations spanning UV to IR wavelengths, are possible for individual stars in our Galaxy or the Magellanic Clouds with new instruments, such as the *Far-Ultraviolet Spectroscopic Explorer* (*FUSE*, Moos et al. 2000).

WR stars in the LMC have been the focus of several spectroscopic investigations. WN stars have been studied by

Send offprint requests to: P. A. Crowther,
e-mail: pac@star.ucl.ac.uk

⋆ Based on observations made with the NASA-CNES-CSA *Far Ultraviolet Spectroscopic Explorer*, and NASA-ESA *Hubble Space Telescope*. Also based on observations collected at the European Southern Observatory in program 63.H-0683, and at the Australian National University Siding Spring Observatory.

Table 1. Observing log for LMC WC4 stars, including narrow-band photometry from Torres-Dodgen & Massey (1988), and catalogue numbers from Breysacher (1981, Br) and Breysacher et al. (1999, BAT).

HD	Br	BAT	v	$b-v$	*FUSE*	*HST*	MSSSO	NTT
32125	7	9	15.02	0.10	–	Sep. 94	Dec. 97	–
32257	8	8	14.89	0.13	–	Nov. 94	Dec. 97	–
32402	10	11	13.89	−0.06	Nov. 01	Apr. 95	Dec. 97	Sep. 99
37026	43	52	14.04	−0.03	Feb. 00	Nov. 94	Dec. 97	–
37680	50	61	14.03	−0.01	Feb. 00	Nov. 94	Dec. 97	–
269888	74	90	15.41	0.19	–	Jun. 95	Dec. 97	–

Conti & Massey (1989), whilst Hamann & Koesterke (1998), and references therein, have determined their quantitative properties, for which a negligible metallicity effect was remarked upon relative to Galactic counterparts (the heavy metal content of the LMC is ∼0.4 $Z_{\odot}$, Dufour 1984). Torres et al. (1986), Smith et al. (1990) and Barzakos et al. (2001) have compared LMC WC stars, with Gräfener et al. (1998) presenting studies of six WC4 stars. In the latter work, WC4 stars were found to possess remarkably uniform (and high) carbon and oxygen abundances, plus a wide range of stellar luminosities. Results were inconclusive whether the mass-loss rates of LMC WC stars are similar to, or lower than, Galactic counterparts. We return to the study of these stars in this paper, since we possess improved and more extensive spectroscopy, including far-UV and near-IR datasets, plus better modelling tools (Hillier & Miller 1998).

We present our new observations in Sect. 2, and discuss the present set of model calculations in Sect. 3. Individual results are presented in Sect. 4 and compared with the previous study of Gräfener et al. Quantitative comparisons are made with Galactic counterparts that have been analysed in a similar manner (Dessart et al. 2000; Hillier & Miller 1999) in Sect. 5, together with evolutionary expectations. Finally, the possibility that WC stars provide the precursors to type Ic SN are discussed in Sect. 6, via the comparison of accurate WC masses with those of the CO-cores determined for recent SN Ic explosions (e.g. Iwamoto et al. 1998, 2000).

2. Observations

For our study, we utilise archival UV *Hubble Space Telescope (HST)* datasets, together with previously unpublished far-UV *FUSE*, optical 2.3 m Mt Stromlo & Siding Spring Observatory (MSSSO) spectroscopy, plus near-IR European Southern Observatory (ESO) New Technology Telescope (NTT) observations, discussed in turn below. An observing log for each of the six program stars, together with photometry from Torres-Dodgen & Massey (1988), is presented in Table 1. Spectral types are WC4 in all cases, following either Smith et al. (1990) or Crowther et al. (1998).

2.1. Far UV spectroscopy

HD 32402, HD 37026, and HD 37680 were observed as part of the *FUSE* Principal Investigator team program to study hot stars (P117, P.I.: J. B. Hutchings) between 2000 February–2001 November, as indicated in Table 1. The spectra were obtained as time-tag mode integrations of 4.5–8.1 ks duration through the 30″ × 30″ (LWRS) aperture. As described by Moos et al. (2000) and Sahnow et al. (2000), *FUSE* data consist of spectra with spectral resolution of ∼15 000 from two Lithium Fluoride (LiF) channels, which cover $\lambda\lambda$990–1187 Å and two Silicon Carbide (SiC) channels, which cover $\lambda\lambda$905–1105 Å. Spectra from each channel were processed by the current version of the standard calibration pipeline (CALFUSE 2.0.5), which corrects for drifts and distortions in the readout electronics of the detectors, removes the effects of thermally induced grating motions, subtracts a background image, corrects for residual astigmatism in the spectrograph optics, and applies flux and wavelength calibrations to the extracted spectra. Spectra from the individual channels were subsequently aligned, merged, and resampled to a constant wavelength step of 0.1 Å in the manner described by Walborn et al. (2002b).

2.2. Near UV spectroscopy

All program stars were observed with the *HST* Faint Object Spectrograph (FOS) instrument between 1994 September–1995 June (PI: D. J. Hillier). Individual exposures were obtained with the G130H, G190H and G270H gratings, respectively, providing complete spectral coverage in the $\lambda\lambda$1140–3301 range. These data have previously been discussed and published in part by Gräfener et al. (1998).

2.3. Optical and far-red spectroscopy

We have used the Double Beam Spectrograph (DBS) at the 2.3 m MSSSO telescope to observe our six targets between 1997 Dec. 24–27. Nearly complete coverage in the optical and far-red region was obtained in two separate exposures, which were in the range 240–1500 s. The dichroic together with the 300 l/mm (blue) and 316 l/mm (red) gratings provided spectroscopy of 3620–6085 Å and 6410–8770 Å, whilst the 600 l/mm (blue) and 316 l/mm (red) gratings permitted observations at 3240–4480 Å and 8640–11 010 Å simultaneously. The detectors for both arms of the DBS were 1752×532 pixel SITE CCD's. A 2″ slit provided a 2 pixel spectral resolution of ∼5 Å, whilst a 6″ slit (for absolute spectrophotometry) provided a spectral resolution of ∼12 Å. A standard data reduction was carried out, including absolute flux calibration, using wide slit spectrophotometry of HD 60753 (B3 IV) and μ Col (O9 V), plus atmospheric correction using B stars HR 2221, 4074 and 4942.

2.4. Near-IR spectroscopy

Long slit, near-IR spectroscopy of HD 32402 was acquired on 1999 Sep. 1–2 with the NTT, using the Son of Isaac (SofI) instrument, a 1024×1024 pixel NICMOS detector, and low resolution IJ (GRB) grating, with spectral coverage 0.94–1.65 μm and a dispersion of 7.0 Å/pix. The 0.6″ slit provided a 2-pixel spectral resolution of 14 Å. The total integration time was

Table 2. Summary of the WC model atom calculations. N_f is the number of full levels, N_s the number of super levels and N_t the corresponding number of transitions. A total of 2526 levels (788 super levels) and 26 239 transitions are considered.

	I			II			III			IV			V			VI			VII			VIII		
Ion	N_f	N_s	N_t	N_f	N_s	N_t	N_f	N_s	N_t	N_f	N_s	N_t	N_f	N_s	N_t	N_f	N_s	N_t	N_f	N_s	N_t	N_f	N_s	N_t
He	39	27	315	30	13	435																		
C				16	9	36	243	100	5513	64	49	1446												
O				29	13	120	154	60	1454	72	30	835	78	41	524	23	17	109						
Ne				48	14	290	101	39	675	68	23	432	117	27	837	34	15	135						
Si										33	23	183												
P										28	16	57	28	18	138									
S										77	29	506	26	14	58	11	7	24						
Ar							36	10	67	105	23	834	61	24	276	81	21	606	37	18	133	12	7	26
Fe										280	21	4223	182	19	2163	190	29	2028	153	14	1216	70	18	483

480 s (1 Sep.) and 960 s (2 Sep.). The removal of atmospheric features was achieved by observing HD 38150 (F8 V) immediately after HD 32402, at a close airmass (within 0.03). Similar observations of Hip 22663 (B2 V) permitted a relative flux correction, using a $T_{\rm eff}$ = 22 kK Kurucz model atmosphere normalized to V = 7.66 mag.

A standard extraction and wavelength calibration was carried out with IRAF, while FIGARO (Shortridge et al. 1999) and DIPSO (Howarth et al. 1998) were used for the atmospheric and flux calibration, first artificially removing stellar hydrogen features from the HD 38150 spectrum. Our relatively fluxed dataset was adjusted to match MSSSO spectrophotometry.

3. Model analysis

3.1. Method

For this study, we employed the code of Hillier & Miller (1998), CMFGEN, which iteratively solves the transfer equation in the co-moving frame subject to statistical and radiative equilibria in an expanding, spherically symmetric and steady-state atmosphere. These models account for clumping, via a volume filling factor, f, and line blanketing, since these effects affect significantly the derived properties of WC stars (e.g. Hillier & Miller 1999). Through the use of "super-levels", extremely complex atoms can been included. For the present application, a total of 2526 levels (combined into 788 super-levels), 40 depth points and 26 239 spectral lines of He, C, O, Ne, Si, S, P, Ar and Fe are considered as indicated in Table 2. The reader is referred to Dessart et al. (2000) for details of the oscillator strengths, collision and photoionization cross-sections. The OPACITY (Seaton 1987, 1995) and IRON projects (Hummer et al. 1993) formed the basis for most atomic data utilised in this work. Test calculations, additionally involving extensive model atoms for Na II-VII, Mg III-VII, Cl IV-VII, Ca IV-IX, Cr IV-VI, Mn IV-VII and Ni IV-IX were also considered, with minor effects on the emergent spectrum, except for an increase in the strength of C IV $\lambda\lambda$1548–51, 5801–12.

Following theoretical discussions by Schmutz (1997), and for consistency with previous studies, we adopt a form for the velocity law (Eq. (8) from Hillier & Miller 1999) such that two exponents are considered (β_1 = 1, β_2 = 20), together with an intermediate ($v_{\rm ext}$) and terminal v_∞ velocity, with $v_{\rm ext} \sim v_\infty - 300$ km s^{-1}. Consequently, acceleration is modest at small radii, and continues to relatively large distances, i.e. $0.9v_\infty$ is reached at $\sim 20R_*$ versus $10R_*$ for a standard β = 1 law. In the future, we intend to relax this assumption via hydrodynamical driving, at least for the outer envelope. Terminal velocities are measured principally from the C IV $\lambda\lambda$1548–51 UV P Cygni profiles, subject to minor adjustment at the line fitting stage, and agree relatively well (within 15%) with previous determinations from Gräfener et al. (1998) who measured wind velocities using the unsaturated C III λ2297 line.

The formal solution of the radiative transfer equation, yielding the final emergent spectrum, is computed separately. Generally, Doppler profiles are adopted throughout, except for C III λ977, C IV $\lambda\lambda$1548–51 for which Voigt profiles are absolutely essential. Except where noted, these final calculations assume $v_{\rm turb}$ = 50 km s^{-1}.

A series of models were calculated for each star in which stellar parameters, T_*, $\log(L/L_\odot)$, $\dot{M}/\sqrt{f}$, C/He and O/He, were adjusted until the observed line strengths and spectroscopic fluxes were reproduced. Our spectroscopic analysis derives $\dot{M}/\sqrt{f}$, rather than $\dot{M}$ and f individually, since line blending is so severe in WC4 stars. This is illustrated in Figs. 1a–c, where we compare selected synthetic line profiles using identical models of HD 32402, except that volume filling factors of f = 1.0, 0.1 and 0.01 are adopted (with corresponding changes in $\dot{M}$). C IV λ7724 is typical of the vast majority of lines, in that solely changes in electron scattering wings are predicted. Emission intensities of some lines, such as $\lambda\lambda$5801–12, are very sensitive to clumping, as are the shapes of the carbon resonance lines C IV $\lambda\lambda$1548–51 and C III λ977. Recall that a Voigt profile is necessary for these lines. It is apparent from Figs. 1d–f that the f = 0.1 case provides the best overall match to observed electron scattering wings, and to the central wavelength of $\lambda\lambda$1548–51, which unusually distinguishes itself as a clumping probe in WC stars in this way.

Hamann & Koesterke (1998) considered clumped models of HD 37026, with f = 1.0, 0.25 and 0.0625, and came to the conclusion that the latter provided the best fit to observations. In general, we can firmly rule out f = 1.0 for all cases, but our (admittedly simplistic) treatment of wind clumping prevents a precise determination – see Dessart & Owocki (2002a,b) for recent progress in this field. Ultimately, we cannot pretend to derive the clumpiness of the wind, and so we have selected

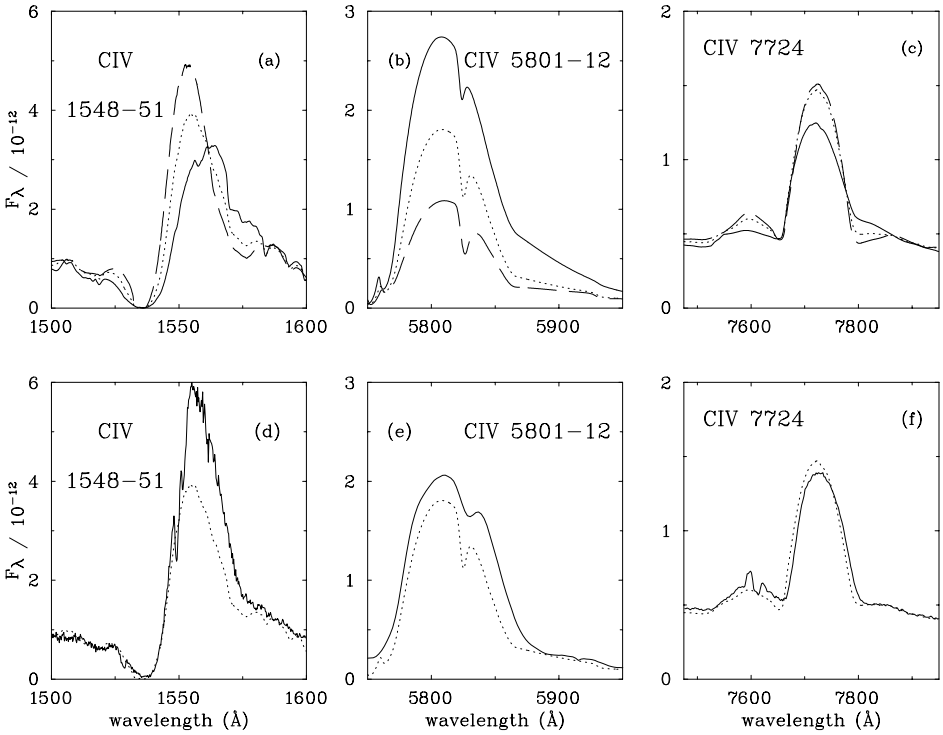

Fig. 1. Panels a–c): synthetic spectra for selected C IV line profiles with parameters $T_\star$ = 90 kK, $\log L/L_\odot$ = 5.70, v_∞ = 3000 km s^{-1}, C/He = 0.14, O/He = 0.02 by number. An unclumped model is shown in solid (f = 1, with $\dot{M}$ = 1.1 × 10^{-4} $M_\odot$ yr^{-1}), moderately clumped as a dotted line (f = 0.1, with $\dot{M}$ = 3.5 × 10^{-5} $M_\odot$ yr^{-1}), and highly clumped as a dashed-line (f = 0.01, with $\dot{M}$ = 1.1 × 10^{-5} $M_\odot$ yr^{-1}. Electron scattering wings, and line intensities for the case of $\lambda\lambda$5801–12, are very sensitive to clumping, as is the shape and location of $\lambda\lambda$1548–51. **Panels d–f):** comparison of moderately clumped (f = 0.1) models with observations of HD 32402, showing generally good agreement. Ordinate units are erg cm^{-2} s^{-1} Å^{-1}.

identical values of f(=0.1) for the other program stars, as a reasonable compromise to the observed spectra in each case, and for consistency with other (Galactic) stars analysed in our previous studies.

3.2. Stellar parameters and abundances

The wind ionization balance is ideally deduced using isolated spectral lines from adjacent ionization stages of helium, carbon or oxygen. In order to ensure consistency with studies that are restricted to optical or far-red wavelengths we selected He I 10830/He II 5412 and C III 6740+8500+9710/C IV 7700. No suitable oxygen diagnostics were available in the optical or far-red, whilst use of He I 10830 was difficult in practise for our program stars (given the poor CCD response in the near-IR), with the exception of NTT-SofI data for HD 32402. Consequently, carbon provided our principal diagnostic lines, with the carbon-to-helium abundance determined from C IV 5471 and He II 5412. We consider the accuracy of our derived luminosities to be 15%, with effective temperatures somewhat worse constrained. Mass-loss rates also have a 15% accuracy if the adopted filling factor if correct.

In Fig. 2 we present de-reddened observations of HD 32125, plus three identical models except that C/He ratios are 0.07, 0.13 (adopted) and 0.21 by number, corresponding to 15%, 25% and 35% carbon by mass, with the oxygen mass fraction maintained at 10%. The relatively small changes in line strength for differing C/He ratios emphasise the need for high S/N and absolute flux calibration. Difficulties are only encountered for stars with very large wind velocities in which C IV 5471 and He II 5412 are severely blended. Overall, we consider an (internal) accuracy of 10% in our derived carbon mass fraction, i.e. 25 ± 3% for the case illustrated above. External errors are difficult to quantify, but from test calculations carried out using the line blanketed code of Gräfener et al. (2002) the degree of consistency is excellent.

In contrast with carbon, the determination of oxygen abundances are much more difficult. This is due to the absence of recombination lines amenable to simple analysis, a much more complex ionization balance structure than He and C, and more problematic line blending – for example the well known oxygen feature between C IV λ5471 and C III λ5696 is almost equally split between O III λ5592 and O V $\lambda\lambda$5572–5607. Nevertheless, there are numerous UV and optical lines of oxygen which are sensitive to abundance variations, which are discussed below for HD 37026. For oxygen we admit an (again internal) accuracy of 50% in our derived oxygen mass fractions. Absolutely, a factor of two is probably a more objective value. Again, test calculations by Gräfener (priv. comm.) indicates good agreement, except for O III lines for which dielectronic contributions to lines differ somewhat.

For elemental species other than He, C and O, we generally adopt 0.4 $Z_\odot$ abundances (Si, S, P, Ar and Fe). We have considered models in which the iron abundance is doubled or halved,

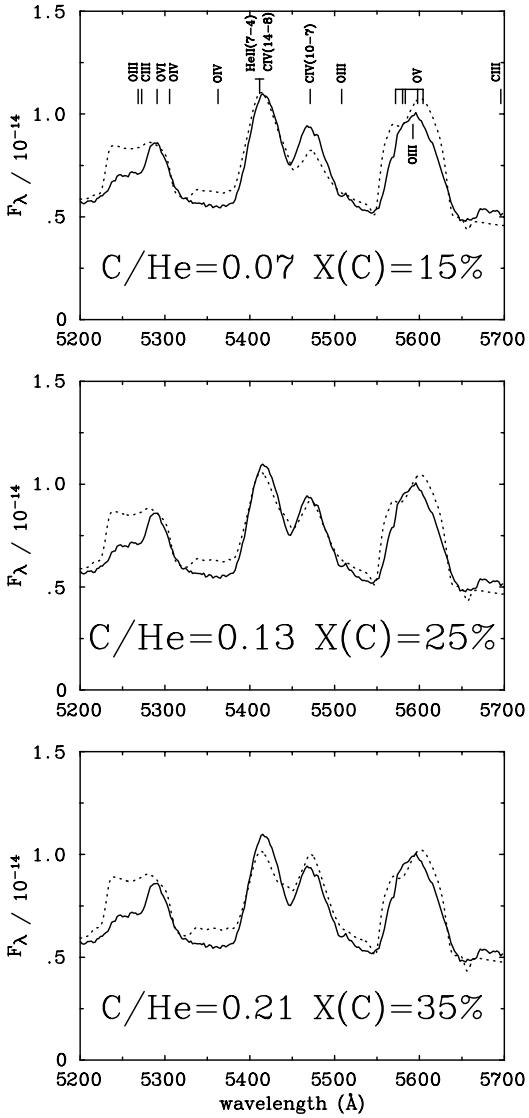

Fig. 2. Comparison between the de-reddened spectroscopy of HD 32125 (solid) in the He II 5412 and C IV 5471 region, and theoretical predictions (dotted). In addition to those features identified ($W_\lambda > 5$ Å), there are numerous weaker carbon, oxygen, neon and sulphur features, From top-to-bottom: C/He = 0.07 by number (15% by mass), 0.13 (25%, adopted) and 0.21 (35%). Ordinate units are erg cm^{-2} s^{-1} Å^{-1}.

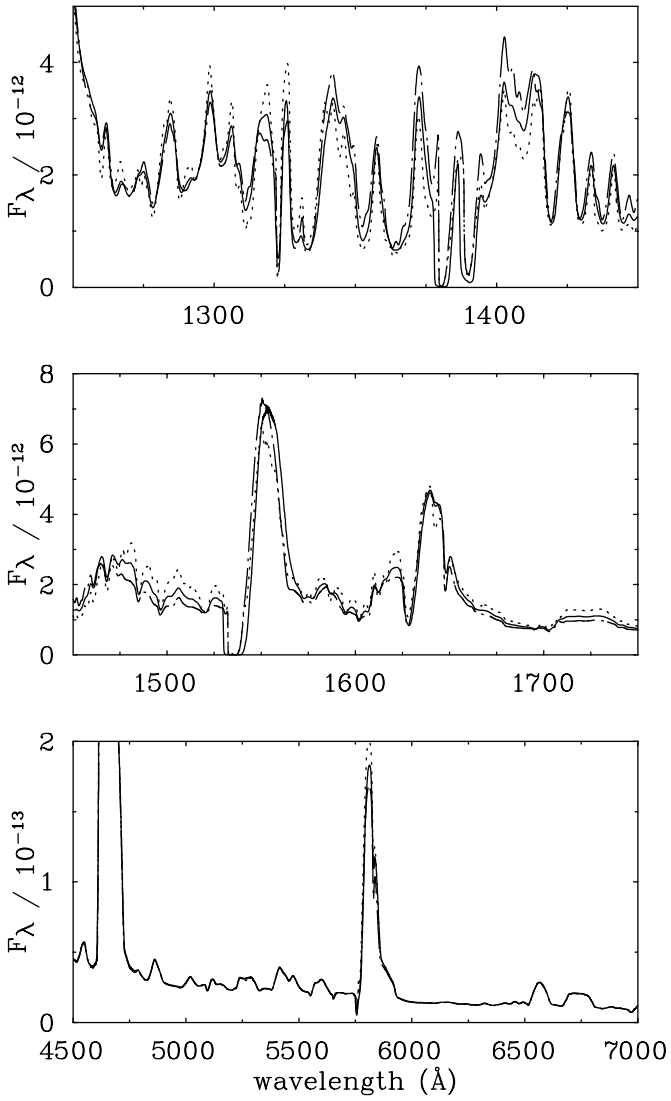

Fig. 3. Comparison between identical synthetic spectra for HD 32402, except that iron abundances are chosen to be 0.2 $Z_\odot$ (dashed) 0.4 $Z_\odot$ (solid) and 0.8 $Z_\odot$ (dotted) This illustrates how difficult it is to accurately determine iron abundances based on UV spectroscopy in WC stars. Differences in iron content within this range has little effect on the emergent carbon-oxygen-helium (diagnostic) lines. Ordinate units are erg cm^{-2} s^{-1} Å^{-1}.

without particularly affecting the emergent spectrum. This is illustrated in Fig. 3 for UV synthetic spectra of HD 32402. For the case of neon, there is observational evidence that Ne is enriched in Galactic WC stars such that its mass fraction is ∼1.5% (Ne/He = 0.004 by number, Dessart et al. 2000). Consequently, we have sought UV/optical line diagnostics as evidence for Ne enrichment in LMC WC4 stars (see below).

3.3. Reddening and distance

Simultaneously with the determination of the ionization balance, wind density and chemistry of each star, the luminosity is adjusted to ensure consistency with de-reddened spectroscopy. In all cases, a Galactic foreground extinction of E_{B-V} = 0.07 is adopted following Schlegel et al. (1998), using the parameterization of Seaton (1979), with $R = 3.1 = A_V/E_{B-V}$. The extinction law followed by Seaton differs substantially from Cardelli et al. (1989) for $\lambda \leq 1500$ Å. The distance modulus to the LMC was assumed to be 18.50, as derived by Cepheids and SN 1987A (Lee et al. 1993; Panagia et al. 1991), corresponding to 50 kpc.

LMC contributions are varied in E_{B-V} and R following the parameterization of Howarth (1983). In the far-UV, interstellar absorption in the H I atomic Lyman series is accounted for following the technique of Herald et al. (2001). Correction for molecular hydrogen in the *FUSE* spectral region has been made by using H_2 column densities determined by Tumlinson et al. (2002): log (H_2/cm^{-2}) = 15.45 and 18.94 for HD 37026 and HD 37680, respectively. The H_2 column density towards HD 32402 is substantial, with log (H_2/cm^{-2}) ∼ 19. HD 37026,

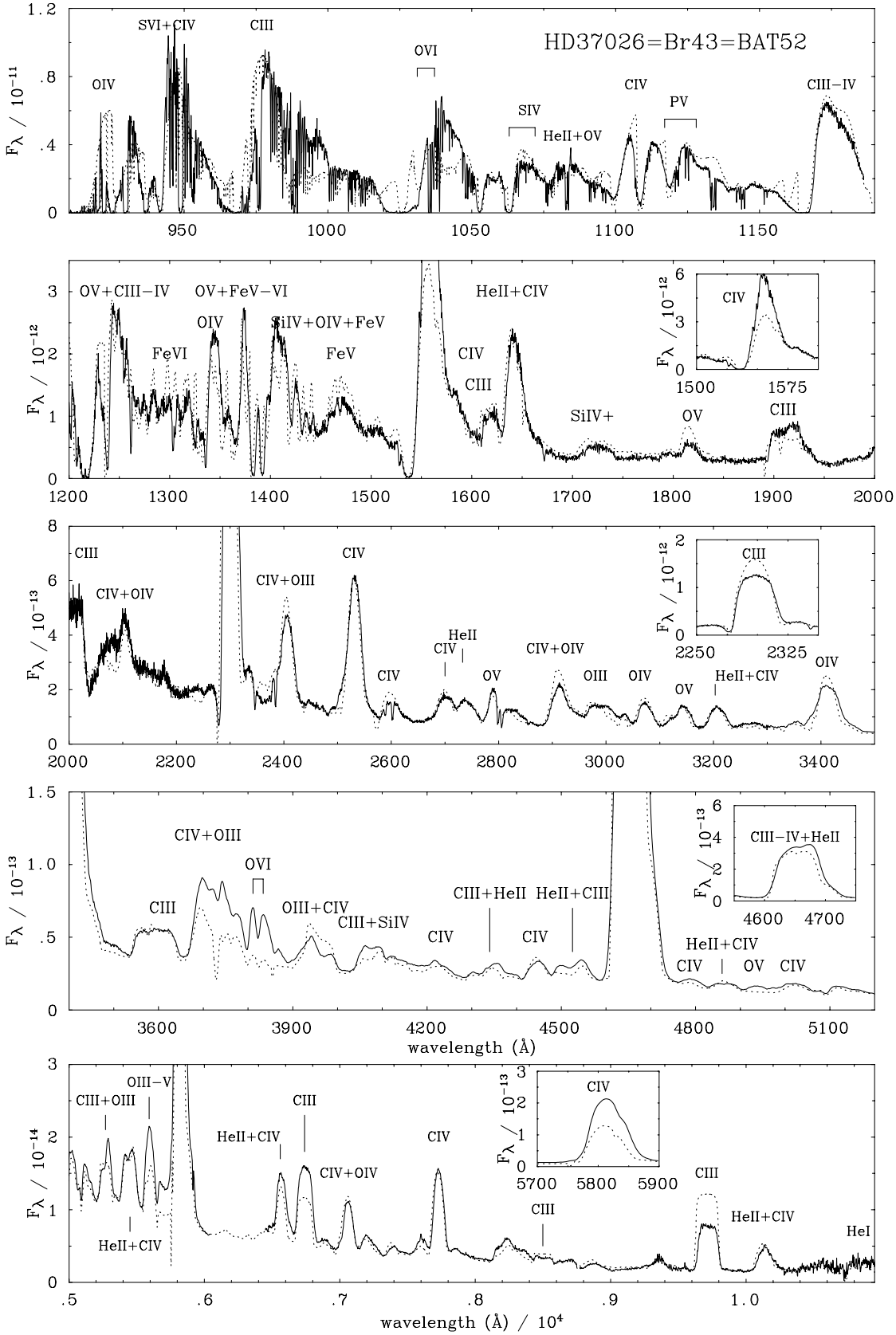

Fig. 4. Comparison between the de-reddened (E_{B-V} = 0.07(Galactic)+0.04(LMC)) flux distribution of HD 37026 (solid) and theoretical predictions (dotted) for $T_\star$ = 90 kK, $\log L/L_\odot$ = 5.65, $\log \dot{M}/(M_\odot\ \mathrm{yr}^{-1})$ = −4.5, v_∞ = 2900 km s^{-1}, C/He = 0.32, O/He = 0.05 by number. For the *FUSE* region, we use an atomic hydrogen column density of $\log N(\mathrm{H/cm}^{-2})$ = 21.0, whilst correction for molecular hydrogen is taken from H_2 models by Tumlinson et al. (2002) using a Doppler width (b = 5.4 km s^{-1}) and total column of $\log(\mathrm{H_2/cm}^{-2})$ = 15.45, considering levels J = 0 to 3. Ordinate units are erg cm^{-2} s^{-1} Å^{-1}, whilst abscissa units are Å except for μm in the bottom panel.

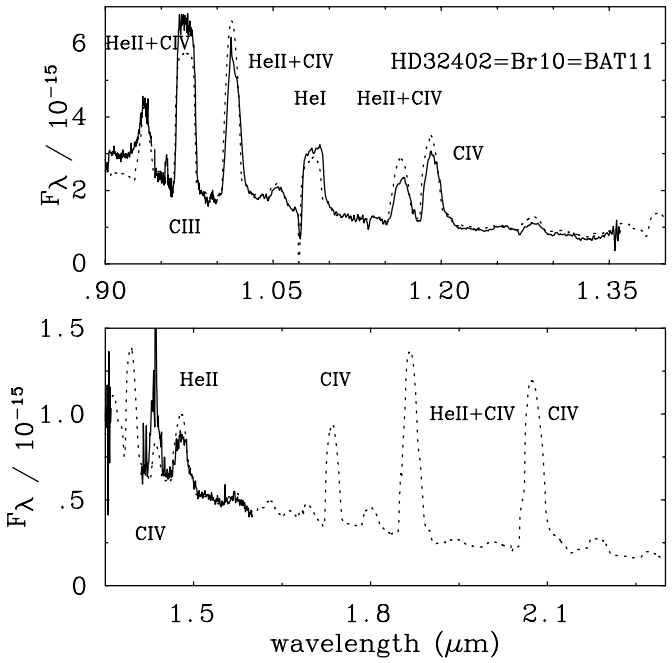

Fig. 5. Comparison between de-reddened near-IR NTT-SofI observations of HD 32402 (solid) and synthetic spectra (dotted) determined from optical diagnostics. Ordinate units are erg cm^{-2} s^{-1} Å^{-1}.

therefore, has by far the "cleanest" far-UV stellar spectrum of the three WC4 stars thus far observed with *FUSE*.

4. Results for individual stars

We have decided against presenting spectral fits for each star in turn, since the model successes and failures are generally common to all our program stars. We solely present spectral fits to the entire far-UV, UV, optical and near-IR observations of one star, HD 37026 in Fig. 4.

4.1. Study of HD 37026 (Brey 43 = BAT99-52)

Overall, the flux distribution of HD 37026 is very well reproduced by the synthetic model – particularly the iron forest in the $\lambda\lambda$1250–1500 region and plethora of near-UV and optical carbon-helium features with C/He = 0.32 by number (44% by mass). He I λ10830 may be rather underestimated in strength, although the low S/N of the observations, due to the poor CCD response beyond 1 μm, hinders detailed comparisons. To illustrate the reliability of near-IR synthetic spectra for WC4 stars based on studies from optical diagnostics we present high S/N NTT-SofI observations of HD 32402 in Fig. 5 with model predictions. Overall the match is excellent, including He I λ10830.

Problematic carbon features for HD 37026 presented in Fig. 4 are as follows. C IV $\lambda\lambda$1548–51 emission is predicted to be somewhat too weak. Previous difficulties with reproducing the C IV $\lambda\lambda$5801–12 feature (e.g. Hillier & Miller 1999) appear to have been mostly resolved by the inclusion of additional metal opacity (specifically Ne and Ar). Unfortunately, C III lines provide conflicting information. For example, λ977, λ1909, λ2297, $\lambda\lambda$4647–50 and λ8500 are reproduced to within 25% in HD 37026. However, λ6470 is up to 50% too weak, whilst λ9710 is similarly too strong. The blend including C III λ3747 is systematically too weak, despite efforts to improve atomic data. Amongst other WC4 stars, consistency between λ6470 and λ9710 is generally excellent.

As introduced above, there are numerous UV and optical lines of oxygen which are sensitive to abundances variations although results are somewhat discrepant. Figure 6 presents identical models for HD 37026 except that the oxygen mass fraction is 5% (O/He = 0.025), 10% (O/He = 0.05) or 20% (O/He = 0.1). Diagnostics which correlate well with abundance are O V λ1815 (indicating 5%), O III λ2983 (10%), O IV λ3072 (~8%), O IV $\lambda\lambda$3560–3 (~8%) and O III+V λ5590 (>20%). It is unfortunate that for HD 37026, the only strong oxygen feature available in the visual implies a substantially different oxygen abundance from the numerous other diagnostics. This is not always the case – λ5590 is representative of near-UV diagnostics for HD 32125, HD 32257 and HD 37680.

Great care should be taken when comparing results from solely optical observations, as is common for extragalactic WC stars (e.g. Smartt et al. 2001), with those additionally including UV and far-UV observations. In the case of HD 37026, we adopt a mean oxygen abundance from the above list of diagnostics, i.e. 9% by mass. The most significant model discrepancy is the predicted strength of the O VI lines – notably $\lambda\lambda$1032–38 (for those stars with far-UV datasets), $\lambda\lambda$3811–34 and λ5290. We have considered the inclusion of X-rays to maintain the population of high oxygen ions in the wind, but without much success, especially for the optical O VI lines. We are only able to maintain such high ions if the wind density were reduced, as for Sand 2 (WO, Crowther et al. 2000), but at the expense of the goodness of fit for other diagnostics.

Whilst the majority of spectral features are from He/C/O/Fe, there are signatures of several other elements in the spectra of WC4 stars. These are most readily apparent from *HST* and *FUSE* observations. Prominent P Cygni profiles of Si IV $\lambda\lambda$1393–1402, P V $\lambda\lambda$1118–28 and S IV $\lambda\lambda$1062–73 features are present, and successfully reproduced with abundances scaled to 0.4 $Z_{\odot}$.

Unfortunately, spectral features of neon (generally Ne III-V) in WC4 stars are rather weak, even for large adopted abundances. This is illustrated in Fig. 7 where UV and optical observations of HD 37026 are compared with models accounting for a varying amount of neon – 2% (dotted), 0.4% (dashed), and 0% (dot-dash). The strongest accessible (unblended) UV features lie in the vicinity of C III λ2297 – Ne IV $\lambda\lambda$2043–73, $\lambda\lambda$2204–21, λ2175, $\lambda\lambda$2351–63, Ne V λ2260. These generally favour a neon abundance of $\leq$0.4%, which still represents a potential overabundance by a factor of $\leq$5. Optical diagnostics are even harder to locate. Ne IV λ5045, λ5245 are amongst the strongest features, but cannot readily be used to determine neon abundances without a superior match to the observed spectrum from other species. We are therefore unable to verify evolutionary predictions for the Ne abundance in WC stars beyond those discussed by Dessart et al. (2000) from mid-IR fine structure lines.

The temperature, density, radius and ionization balance of He, C, O, Ne and Fe for our final HD 37026 model versus wind

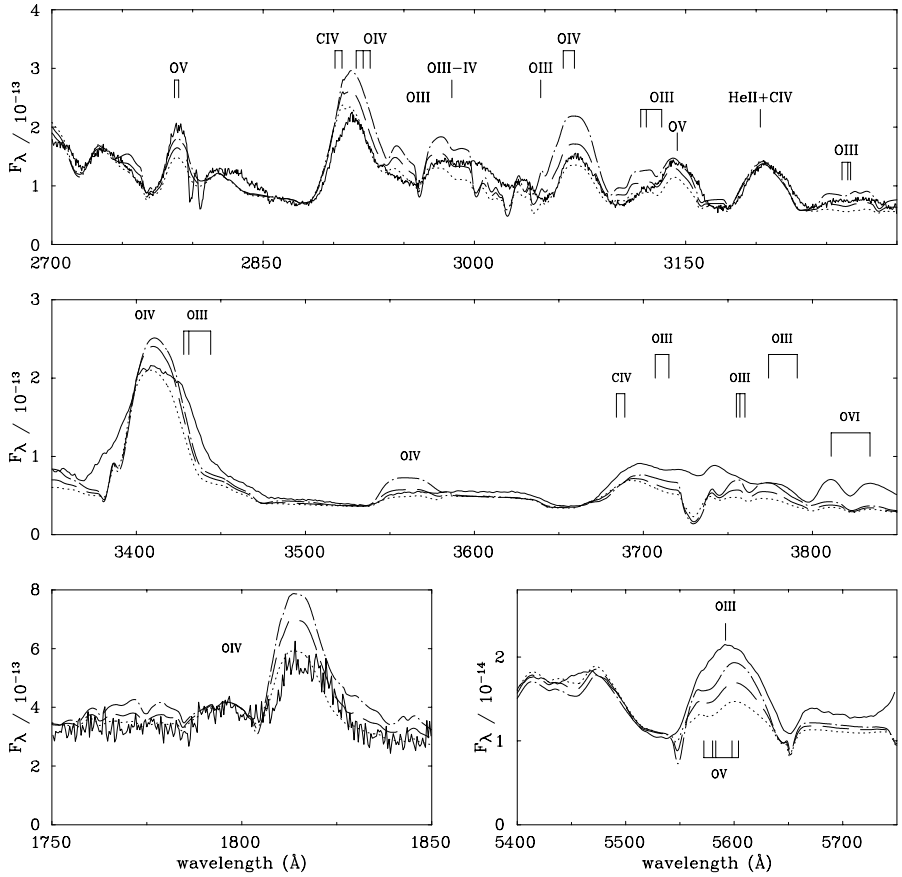

Fig. 6. Comparison between de-reddened observations of HD 37026 (solid) and synthetic spectra for a variety of oxygen abundances – 5% by mass (dotted), 10% (dashed) and 20% (dot-dash) O IV $\lambda\lambda$3403–13 is rather insensitive to abundance, whilst the strong λ2900 feature is a blend of C IV λ2906, 2918 and O IV λ2921. Ordinate units are erg cm^{-2} s^{-1} Å^{-1}.

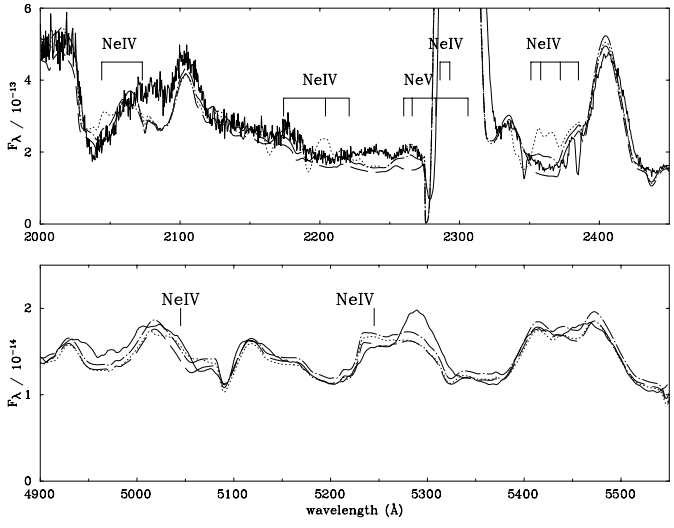

Fig. 7. Comparison between de-reddened observations of HD 37026 (solid) and synthetic spectra for a variety of neon abundances – 2% by mass (dotted), 0.4% (dashed), and 0% (dot-dashed). Ordinate units are erg cm^{-2} s^{-1} Å^{-1}.

velocity are presented in Fig. 8. This illustrates the complex ionization structure for heavy elements with respect to helium and carbon.

4.2. Summary of results and comparison with Gräfener et al.

Deduced stellar properties for each star are presented in Table 3, including ionizing fluxes below the H I (Q_0), He I (Q_1), and He II (Q_2) edges. We also present final synthetic spectra with each observation for the diagnostic He II 5412 and C IV 5471 profiles in Fig. 9.

The present sample of stars has previously been studied by Gräfener et al. (1998), whilst Hamann & Koesterke (1998) have considered clumped models for HD 37026. We present a comparison of the derived parameters from these various studies in Table 4. Overall, we obtain similar stellar temperatures to Gräfener et al., but substantially higher stellar luminosities (0.1–0.4 dex), lower wind densities (0.2 ± 0.1 dex, *after* correcting for the clumped wind) and higher wind velocities (up to ~15%). We concur with Gräfener et al., in that LMC WC4 stars form a relatively homogeneous sample, with high luminosities, temperatures and comparable wind densities. However, our improved observational and theoretical approach has led to substantially revised stellar parameters, notably relating to chemical abundances. Our improved optical spectroscopy permits a much finer determination of C/He ratios, e.g. for HD 37680 we obtain C/He = 0.10 by number versus C/He = 0.27 according to Gräfener et al. – see Fig. 9.

Table 3. Stellar parameters for the program LMC WC4 stars, plus Sand 2 (WO) from Crowther et al. (2000) analysed in the same manner. Note that all models assume a filling factor, f, of 0.1, whilst a two-component velocity law was used in all cases with $\beta_1 = 1, \beta_2 = 20$, $v_{\rm ext} = (v_\infty - 300)$ km s^{-1}.

HD	T_* kK	R_* $R_\odot$	log $L_{\rm ph}$ $L_\odot$	$T_{2/3}$ kK	$R_{2/3}$ $R_\odot$	log $\dot{M}$ $M_\odot$ yr^{-1}	v_∞ km s^{-1}	log Q_0 s^{-1}	log Q_1 s^{-1}	log Q_2 s^{-1}	C/He	O/He	$\beta_{\rm He}$ %	$\beta_{\rm C}$ %	$\beta_{\rm O}$ %
32125	90	2.2	5.44	74	3.2	−4.8	2500	49.32	48.91	39.03	0.13	0.04	65	25	10
32257	85	2.3	5.42	71	3.4	−4.9	2300	49.29	48.81	36.25	0.35	0.04	45	47	8
32402	90	2.9	5.70	67	5.2	−4.5	3000	49.55	49.10	36.11	0.14	0.02	66	28	5
37026	90	2.8	5.65	68	4.8	−4.5	2900	49.51	48.98	38.80	0.32	0.05	46	44	9
37680	85	3.2	5.68	62	6.0	−4.4	3200	49.53	49.04	38.36	0.10	0.01	74	22	3
269888	85	2.4	5.44	72	3.4	−4.8	2600	49.31	48.86	36.27	0.32	0.06	45	43	11
Sand 2	150	0.65	5.28	110	1.2	−4.9	4100	49.10	48.85	40.31	0.70	0.15	27	56	16

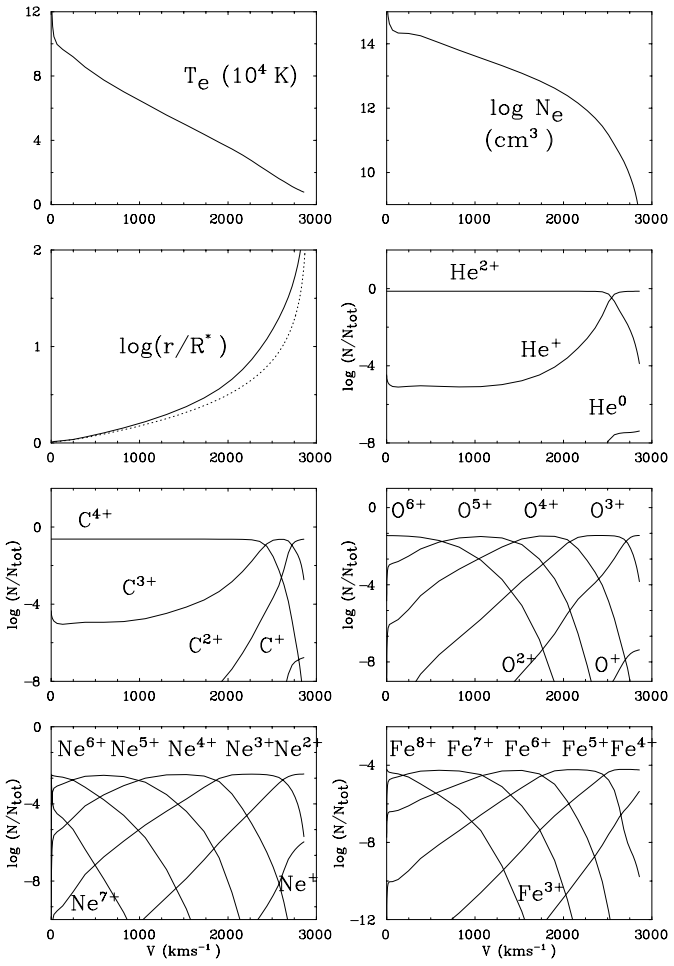

Fig. 8. Atmospheric structure of our final HD 37026 model, indicating the variation of temperature (10^4 K), density (cm^{-3}) and radius (R_*) with velocity (km s^{-1}), plus the ionization balance (in $N/N_{\rm tot}$) for helium, carbon, oxygen, neon and iron. A standard $\beta = 1$ velocity law is also included on the radius plot (dotted line).

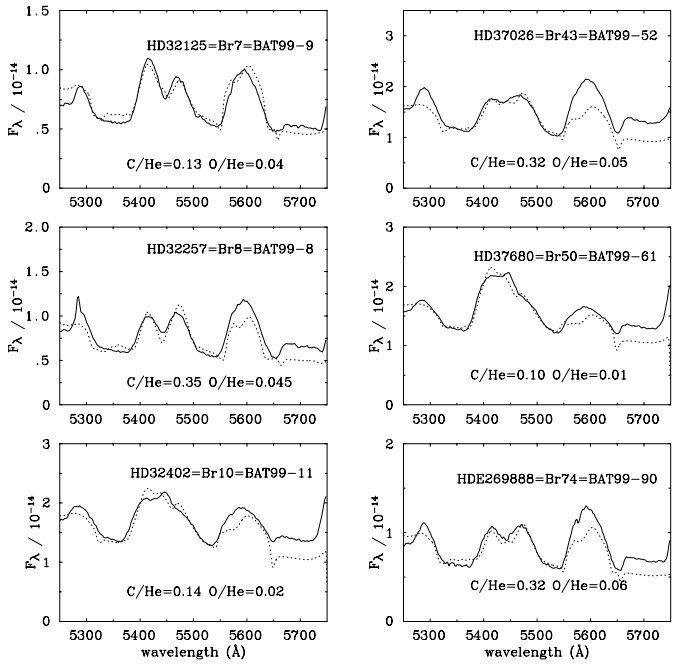

Fig. 9. Comparison between the de-reddened spectroscopy of the targets (solid) in the He II 5411, C IV 5471 and O III-V 5590 region, and final theoretical predictions (dotted), demonstrating the excellent agreement reached for C/He determinations. Ordinate units are erg cm^{-2} s^{-1} Å^{-1}.

Differences between the two methods are as follows:

1. Observationally, Gräfener et al. utilised identical *HST*/FOS UV spectroscopy, plus 10–15 Å resolution optical datasets from Torres & Massey (1987) covering $\lambda\lambda$3375–7375, with the exception of HD 32402 for which they had higher quality ESO spectra. In all cases their observations omitted the useful far-red MSSSO and far-UV *FUSE* diagnostics;
2. Theoretically, similar model assumptions were made by Gräfener et al., except that relatively simple model atoms of helium, carbon and oxygen were used (e.g. O III was omitted). We deduce substantially lower O/He ratios (<0.1) than Gräfener et al. (0.05–0.25), plus a lower range of C/He ratios due to our improved optical spectroscopy (0.1–0.35 versus 0.3–0.55) and our strict adherence to He II 5412/C IV 5471 as abundance diagnostics, plus the allowance for clumping. It is possible that erroneous C/He abundances may be derived if the He II 5412 electron scattering wing is unrealistically strong;

Table 4. Quantitative comparison between fundamental stellar parameters newly derived here for LMC and (selected) Galactic WC stars (referred to as C02) – using line blanketed, clumped models of Hillier & Miller 1998) – and by Gräfener et al. (1998, G98) and Koesterke & Hamann (1995, KH95) using non-blanketed homogeneous models, and Hamann & Koesterke (1998 HK98) using non-blanketed clumped models for HD 37026. Catalogue number for LMC (BAT: Breysacher et al. 1999) and Galactic (WR: van der Hucht 2001) stars are indicated in parenthesis.

HD	$T_\star$	$\log L_{\rm ph}$	$\log\left(\frac{\dot{M}}{\sqrt{f}}\right)$	v_∞	C/He	O/He	D	Ref
	kK	$L_\odot$	$M_\odot\,{\rm yr}^{-1}$	km s^{-1}			kpc	
				LMC				
32125	90	5.44	−4.3	2500	0.13	0.04	50	C02
(9)	95	5.29	−4.2	2300	0.32	0.12	50	G98
32257	85	5.42	−4.4	2300	0.35	0.05	50	C02
(8)	104	5.13	−4.1	2300	0.43	0.24	50	G98
32402	85	5.70	−4.0	3000	0.14	0.02	50	C02
(11)	92	5.62	−3.8	2800	0.55	0.16	50	G98
37026	90	5.65	−4.0	2900	0.32	0.05	50	C02
(52)	103	5.26	−3.9	2600	0.43	0.24	50	G98
	141	5.6	−3.7	2800	0.43	0.24	50	HK98
37680	85	5.68	−3.9	3200	0.10	0.01	50	C02
(61)	94	5.55	−3.7	2800	0.27	0.05	50	G98
269888	85	5.44	−4.3	2600	0.32	0.06	50	C02
(90)	104	5.13	−4.1	2300	0.43	0.24	50	G98
				Galactic				
76536	80	5.38	−4.2	2055	0.25	0.03	2.0	C02
(14)	86	4.9	−4.2	1800	0.14	–	2.0	KH95
213049	80	5.02	−4.5	2280	0.30	0.04	2.7	C02
(154)	71	4.9	−4.2	2050	0.22	–	3.5	KH95

3. Line blanketing was neglected by Gräfener et al., as was the contribution to the opacity by iron and other heavy elements. In contrast, we account for Ne, Si, P, S, Ar and Fe, and also consider the (minor) influence of other heavy elements. The neglect of blanketing, and use of restricted model atoms yields erroneous rectified synthetic spectra both in the UV (due to the iron forest) and the optical (due to many broad overlapping features), see Hillier & Miller (1998, 1999);
4. Iron line blanketing is principally responsible for the increased stellar luminosities obtained here relative to Gräfener et al. We obtain bolometric corrections in the range $-4.8 \leq$ B.C. ≤ -4.5 mag, up to 0.5 mag greater than WC6–8 stars, but 1 mag lower than Sand 2 (Crowther et al. 2000). We also derive somewhat higher interstellar reddenings to the program stars than Gräfener et al. via our spectral synthesis, typically by $A_V \sim 0.2$ mag as presented in Table 5, owing to the superior technique followed.

Recently, Gräfener et al. (2002) presented a line blanketed study of HD 165763 (WC5) where many of their previous deficiencies are rectified, i.e. enhanced model atoms for carbon and oxygen, line blanketing from iron group elements, clumping, and a more objective line profile fitting technique. Indeed, test calculations carried out by Gräfener (priv. comm.) for HD 37026 show excellent consistency with the present results, giving confidence in results obtained with the two independent codes.

Whilst Gräfener et al. included the opacity from other iron group elements, Ne ... Ar were omitted. We find that additional opacity sources (namely Na, Mg, Cl, Ca, Cr, Mn, Ni) play negligible spectroscopic role, other than a strengthening of C IV $\lambda\lambda$1548-51, $\lambda\lambda$5801–12 emission, but do contribute to the line driving force[1]. From test calculations, the inclusion of these additional lines does help, but the effect is still insufficient to supply the necessary driving force, especially in initiating the outflow at the base of the wind, in common with Gräfener et al. (2002). This will be discussed in a forthcoming publication.

5. Comparison with properties of Galactic WC stars

We have presented a detailed study of six LMC WC stars. How do their properties compare with Galactic counterparts? What differences/similarities might be expected from evolutionary predictions?

It is well known that WC4 stars are relatively rare in the Milky Way, with only 5 known out of 87 WC stars (van der Hucht 2001), whilst they dominate the LMC carbon sequence with 15 known out of 23 WC stars (Breysacher et al. 1999). Indeed, most LMC WC stars with WC5–6 spectral types are WC4+O binaries with the later apparent subtypes resulting from C III λ5696 emission due to wind collision (Bartzakos et al. 2001).

5.1. New analyses of Galactic WC stars

It is unfortunate that only a few Galactic WC stars lie at known distances. There are no single cluster/association WC4 stars, so we are unable to directly compare our LMC results with Galactic counterparts. Instead, comparisons must be made with WC5–8 stars, which have been analysed in a similar manner, namely γ Vel (WR11, WC8+O, De Marco et al. 2000); HD 92908 (WR23, WC6, Smartt et al. 2001), HD 165763 (WR111, WC5, Hillier & Miller 1999), and HD 192103 (WR135, WC8, Dessart et al. 2000). To this short list we have added HD 156385 (WR90, WC7) for which Dessart et al. (2000) obtained a distance based on a calibration of (binary) WC7 cluster/association members.

In order to produce a more substantial set of data for Galactic WC stars, we have newly analysed two stars whose distances are known from OB association membership – HD 76536 (WR 14, WC7) and HD 213049 (WR 154, WC6). Spectrosopic observations, cluster distances and derived reddenings are listed in Table 6. Ultraviolet datasets generally represent low dispersion *International Ultraviolet Explorer (IUE)* spectroscopy, with the exception of three (merged) high dispersion short wavelength (SWP) observations of HD 76536.

[1] These additional elements are omitted from our present analysis for consistency with our recent studies of Galactic WC stars (e.g. Dessart et al. 2000).

Table 5. Interstellar reddenings, absolute magnitudes, and H I column densities (from fits to Lyα) to the program LMC WC4 stars, adopting a mean Galactic foreground of E_{B-V} = 0.07 from Schlegel et al. (1998). Narrow-band photometry is taken from Torres-Dodgen & Massey (1988), whilst we include comparisons with previous reddening determinations by Gräfener et al. (1998) and Morris et al. (1991).

HD	v	E_{B-V}(Gal + LMC)			log N(H I)	M_v
	mag	This work	Gräfener et al.	Morris et al.	cm^{-2}	mag
32125	15.02	0.07+0.09	0.03+0.08	0.01	21.5	−4.02
32257	14.89	0.07+0.08	0.03+0.06	0.08	21.0	−4.12
32402	13.89	0.07+0.04	0.03+0.05		21.0	−5.00
37026	14.04	0.07+0.04	0.03+0.01	0.08	21.0	−4.85
37680	14.03	0.07+0.06	0.03+0.05	0.05	21.3	−4.92
269888	15.41	0.07+0.27	0.03+0.28		22.0	−4.19

Table 6. Observing log for Galactic WC stars, including narrow-band photometry from Torres-Dodgen & Massey (1988), catalogue numbers and cluster/association distances from van der Hucht (2001). Optical spectrophotometry for HD 213049 is taken from Torres & Massey (1987).

HD	WR	Sp type	*IUE*	MSSSO/ KPNO	v mag	d kpc	E_{b-v} mag	M_v mag
76536	14	WC7	Sep 80	Dec 97	9.42	2.0	0.61	−4.6
213049	154	WC6	May 82	Oct 80	11.54	2.7	0.72	−3.6

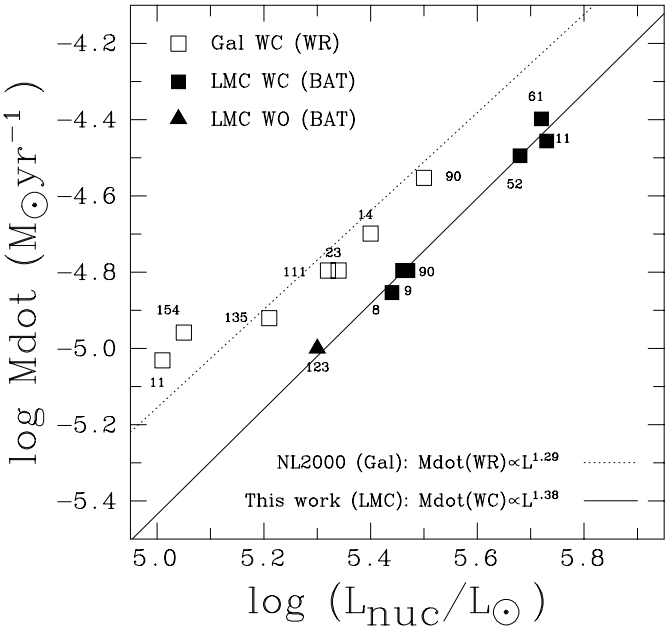

Fig. 10. Comparison between the mass-loss rates and luminosities of LMC WC4 (filled squares), WO stars (filled triangle, Crowther et al. 2000) and Galactic WC5-8 stars (open squares) at known distances. The lines correspond to the calibrations of Nugis & Lamers (2000) for Galactic WR stars (dotted), assuming C/He = 0.2, C/O = 4 by number, plus a linear fit to the LMC WC and WO results (solid).

Optical datasets are drawn from Mt Stromlo 2.3 m DBS observations, obtained during our LMC Dec. 1997 observing campaign for HD 76536, plus archival Torres & Massey (1987) datasets for HD 213049 obtained with the 0.9 m Kitt-Peak (KPNO) intensified Reticon scanner (IRS). We obtain somewhat higher reddening determinations than the recent literature (Koesterke & Hamann 1995; Morris et al. 1993) for HD 76536 and HD 213049, namely E_{b-v} = 0.42–0.49 and 0.63–0.68, respectively.

Identical analysis methods were employed to those presented above. For conciseness, we omit presenting fits to spectral lines for HD 76536 and HD 213049, although the quality is comparable with those of HD 156385 (WC7, Dessart et al. 2000) and HD 92809 (WC6, Smartt et al. 2001). Note that earlier problems with reproducing the strength of C III λ4186 have been resolved and were caused by a "poor" super-level assignment.

We present derived stellar parameters in Table 4, together with those obtained using non-blanketed helium-carbon models by Koesterke & Hamann (1995). The use of blanketed model atmospheres result in higher stellar luminosities as has been discussed above for the LMC WC4 stars, whilst mass-loss rates are again reduced even after correcting for clumping. C/He ratios are increased in this case, although Koesterke & Hamann (1995) neglected oxygen in their calculations.

5.2. A metallicity effect?

In Fig. 10 we compare the luminosities and mass-loss rates of LMC WC stars with Galactic counterparts located at known distances, including HD 76536 and HD 213049 for the first time. Observationally, two main effects are apparent:

- It is striking that the *mean* luminosity of WC stars in the LMC, log($L/L_\odot$) = 5.6, is a factor of two times higher than those of their Galactic counterparts, log($L/L_\odot$) = 5.3, which have been studied in an analogous manner. The conventional interpretation of this difference is that LMC stars are descended from, on average, higher initial mass stars, as might be expected from evolutionary predictions that account for the lower mass-loss rates during the main-sequence and post main-sequence phases at lower metallicities. A more speculative alternative is that their initial masses span a similar range, but that they are currently faster rotators owing to lower mass-loss rates during earlier evolutionary phases. Polarization evidence points to the majority of Galactic WC stars being fairly symmetric, and hence are slow rotators by inference (Harries et al. 1998);
- LMC WC stars possess lower mass-loss rates than Galactic stars of similar luminosity, unless clumping factors differ between the two samples. The semi-empirical calibrations of Nugis & Lamers (2000) for Galactic WR stars match the observed WC properties rather well, whilst a linear fit to the LMC WC and WO data reveals

$$\log(\dot{M}) = 1.38 \log(L/L_\odot) - 12.35 \quad (1)$$

with a similar slope to the Nugis & Lamers (2000) generic WR calibration (their Eq. (22)), albeit offset by ∼0.2 dex.

The metallicity dependence of the mass-loss rate for O stars ($\dot{M} \propto Z^{0.5-0.7}$) is well established observationally

(Puls et al. 1996) and theoretically (Kudritzki & Puls 2000; Vink et al. 2001). The situation for WN stars is less clear (Crowther 2000; Hamann & Koesterke 2000). However, since iron group elements provide most of the driving for the winds of WN stars, they should exhibit a similar dependence on metallicity as the O-type stars. A metallicity dependence of $\sim Z^{0.5}$ would predict that LMC WR stars have winds that are 0.2 dex lower than equivalent Galactic stars, as appears to be the case.

One might question whether a metallicity dependence of WC stars is expected, since their winds are so dominated by carbon and oxygen. From test calculations for WC4 stars, we find that the contribution of lines from dominant ions (~250 eV) at the base of the wind (<100 km s^{-1}) is crucial to initiating the outflow. Carbon does not possess lines from such ions since the ionization potential of C^{3+} (64 eV) and C^{4+} (392 eV) do not lie in the necessary range – the same is true of oxygen (recall Fig. 8). Instead, ions from Ne, Ar, and Fe-group elements appear to be critical in initiating the outflow from early-type WC stars, which would qualitatively explain their sensitivity to heavy metal content.

We shall see in the next section that a metallicity dependence of mass-loss rates contributes to an explanation for the subtype distribution amongst WC stars. In addition, since weaker WR winds are more transparent to harder ionizing photons (Schmutz et al. 1992; Crowther 1999) one would expect a greater contribution of WR stars to the hard ionization of young starburst regions in more metal deficient galaxies. The inclusion of line blanketed metallicity dependent mass-loss rates for WR stars in evolutionary synthesis calculations is discussed by Smith et al. (2002).

The Galactic and LMC WC populations are further compared in Fig. 11, where we present their (C+O)/He values versus luminosity, together with evolutionary predictions for non-rotating stars (solid, Meynet et al. 1994) for the two metallicities, plus results for an initially rapidly rotating 40 $M_\odot$ model at 1.0 $Z_\odot$ (dotted, Meynet & Maeder 2000). It is apparent that these stars reveal similar surface enrichments, despite their differences in spectral types (Galactic: WC5–8; LMC: WC4) and stellar luminosities. The shift to (observed) higher luminosity is reasonably well reproduced in the non-rotating evolutionary models, although the shift in the (sole) rotating track is dramatic. Therefore, we must await results for a wider initial range of masses and rotational velocities before we can have confidence in the validity of these predictions.

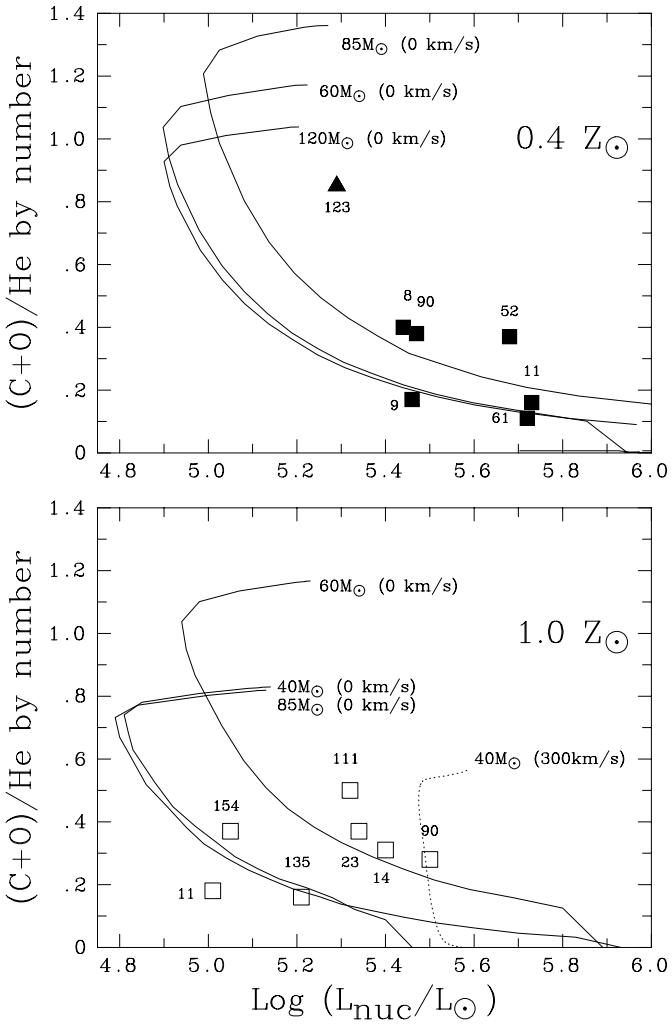

Fig. 11. Comparison between the (C+O)/He values of WC stars in the LMC and Galaxy versus stellar luminosity, together with evolutionary predictions for non-rotating stars (Meynet et al. 1994) for the two metallicities, plus results from an initially rotating 40 $M_\odot$ solar metallicity model from Meynet & Maeder (2000). Symbols (and BAT/WR numbers) are as for the previous figure.

5.3. Differences in WC spectral types between Galactic and LMC stars?

While we have established that WC stars in the LMC are typically more luminous, and possess lower mass-loss rates than Galactic counterparts, what is the origin of their systematically earlier spectral types? This has been assumed to be due either to temperature differences and/or an abundance effect.

Smith & Maeder (1991) adopted the hypothesis that the difference between the WC subtypes was primarily governed by a variable surface abundance ratio, (C+O)/He. This was based on recombination line studies of a sample of Galactic WC4–9 stars. However, only a single WC4 star was included in their sample, whilst recombination studies of late-type WC stars are fraught with difficulties (Hillier 1989). The present results reveal further that the expected (C+O)/He ratios for WC4 stars (0.7–1.0) are not supported here (0.1–0.4), with all Galactic and LMC WC stars poorer in carbon and oxygen than standard (non-rotating) evolutionary models would suggest.

With regard to oxygen abundances, evolutionary predictions for non-rotating massive stars indicate O/C = 0.1–0.22 by number at the stage in which 0.1 ≤ C/He ≤ 0.3, in good agreement with O/C = 0.1–0.25 determined here. Predictions from evolutionary models in which rotation is considered (albeit for solar abundances only) indicate a fairly similar range (O/C = 0.2–0.3 by number).

Crowther (1999) proposed that the variety of early-type WC subtypes results principally from differing wind densities,

rather than surface abundances or ionization. This seems to be supported in Fig. 10. We have further illustrated this effect in Fig. 12 where we present UV and optical observations of HD 156385 (WC7, Galactic) and HD 32257 (WC4, LMC). Clearly these distinct spectral types do not differ dramatically in their optical spectrum, other than the strength of the C III classification diagnostic at λ5696. Hillier (1989) first emphasised the sensitivity of this line to stellar parameters, owing to the alternative decay mechanism from the upper level to 574 Å with a branching ratio of ~150. Consequently, λ5696 will only be strong when λ574 has a large optical depth. Note that other C III lines, for instance the feature at λ6740, do not differ significantly between the two stars. Conti et al. (1990) has previously remarked upon how other strong C III lines (λ4650, λ9710) do not closely follow the classification C III line. In addition, the He II λ5412–C IV λ5471 blend is remarkably similar for these two stars, such that their C/He abundances are essentially identical.

We include synthetic spectra for HD 32257 (from the present work) in Fig. 12, plus two further models in which changes to the temperature and mass-loss rate are made. The temperature is reduced from 85 kK to 80 kK, and then to 75 kK, whilst the mass-loss rate is increased from 1.5×10^{-5} $M_\odot$ yr^{-1}, to 2.1×10^{-5} $M_\odot$ yr^{-1}, and then to 2.8×10^{-5} $M_\odot$ yr^{-1}, in order to closely match the parameters determined by Dessart et al. (2000) for HD 156385. From the figure, it is apparent that this small shift in parameters is sufficient for the spectral type to shift from WC4 to WC7, whilst other C III lines remain remarkably stable. Stellar temperature certainly plays a role – fixing the mass-loss rate and increasing the luminosity at constant radius also reduces the strength of λ5696. In the UV, the effect of varying wind density is also evident. For example, the higher mass-loss rate of HD 156385 dramatically weakens C IV $\lambda\lambda$1548–51 through iron-group blanketing.

From Fig. 12 one might presume that mass-loss plays a principal role in determining spectral types for all WC stars, via the effect on C III λ5696, However this is not always the case. It has been established for several decades that early-type WC stars possess broader lines than late-type WC stars. Whatever its physical origin, this also has the effect of weakening the classification C III λ5696 line. From recent, mostly unpublished calculations, it is apparent that WC8 and especially WC9 stars do have significantly lower stellar temperatures than other WC subtypes. Wind density does appear to play the principal role amongst WC4–7 stars, because of the sensitivity of the classification C III λ5696 line to mass-loss rate. Therefore, the spectral type amongst WC4–7 stars, which we consider to represent "early-type" WC stars is principally defined by wind density, with temperature a secondary effect and no role played by carbon abundance. WC4 and WO stars *definitely* possess weaker winds than other WCE stars, and *probably* have the highest stellar temperatures. Most likely, weaker winds *and* higher temperatures distinguishes WO stars from WC4 subtypes.

In comparison, the classification criteria for WN stars are much stronger indicators of ionization than those of WC stars. The sole exception is that N IV λ4058/N III λ4634–41 is sensitive to nitrogen abundance at fixed temperature, as illustrated by Crowther (2000). This ratio now forms the basis for classification of early O stars (Walborn et al. 2002a).

Table 7. Determinations of masses for Galactic and LMC WC stars using the relationship from Langer (1989) for stellar (photon) luminosities ($M_{\rm L89}$). Correction for wind blanketing effects discussed by Heger & Langer (1996) imply slightly higher (nuclear) luminosities ($L_{\rm nuc}$) and masses ($M_{\rm nuc}$). We also provide predicted final pre-SN masses ($M_{\rm pre-SN}$) based on estimates of lifetimes (τ) remaining, using alternative evolutionary models – Meynet et al. (1994, 0.4 $Z_\odot$ and 1.0 $Z_\odot$) or Meynet & Maeder (2000, 1.0 $Z_\odot$) as discussed in the text, plus the time dependent mass-loss rates scaled according to Eq. (1). Stellar properties for Galactic stars are taken from Hillier & Miller (1999), Dessart et al. (2000), De Marco et al. (2000), Smartt et al. (2001).

HD	$\log \frac{L_{\rm ph}}{L_\odot}$	$\log \frac{L_{\rm nuc}}{L_\odot}$	$\frac{M_{\rm L89}}{M_\odot}$	$\frac{M_{\rm nuc}}{M_\odot}$	τ 10^5 yr	$\dot{M}$ 10^{-5} $M_\odot$ yr^{-1}	$M_{\rm pre-SN}$ $M_\odot$
32125	5.44	5.46	14.6	14.8	3.7	1.6–0.7	11.1
(WC4)					0.9	1.6–1.2	13.7
32257	5.42	5.44	14.3	14.3	2.7	1.4–0.8	11.8
(WC4)					0.5	1.4–1.2	14.0
32402	5.70	5.73	20.4	21.2	4.0	3.5–1.1	13.8
(WC4)					1.0	3.5–2.4	18.7
37026	5.65	5.68	19.1	19.8	2.9	3.2–1.3	14.1
(WC4)					0.6	3.2–2.5	18.2
37680	5.68	5.72	19.9	20.9	4.5	4.0–0.9	12.2
(WC4)					1.1	4.0–2.5	17.5
269888	5.45	5.47	14.8	15.0	2.7	1.6–0.8	12.1
(WC4)					0.5	1.6–1.4	14.4
68273	5.00	5.01	8.9	8.7	3.9	0.9–0.4	6.5
(WC8)					0.9	0.9–0.7	8.1
76536	5.38	5.40	13.6	13.7	3.0	2.0–0.8	9.7
(WC7)					0.7	2.0–1.6	12.4
92809	5.32	5.34	12.7	12.7	2.5	1.6–0.8	9.8
(WC6)					0.5	1.6–1.4	12.0
156385	5.48	5.50	15.4	15.5	3.0	2.5–1.0	10.6
(WC7)					0.7	2.5–2.0	13.9
165763	5.30	5.32	12.4	12.5	1.8	1.6–0.9	10.1
(WC5)					0.1	1.6–1.6	12.3
192103	5.20	5.21	11.0	10.9	4.1	1.2–0.5	7.9
(WC8)					1.0	1.2–0.9	10.0
213049	5.02	5.05	9.1	9.1	2.5	1.2–0.6	7.0
(WC6)					0.5	1.2–1.0	8.5

6. Wolf-Rayet masses

6.1. Present and final masses of WC stars

Present LMC WC4 masses can be calculated based on their stellar luminosities, according to Schaerer & Maeder (1992) or Langer (1989), revealing values in the range 12–18 $M_\odot$. However, these calculations neglect the fact that measured (photon) luminosities in WR stars will be less than that generated by nuclear processes in the deep interior, the so-called "wind darkening" effect. Taking wind darkening into account

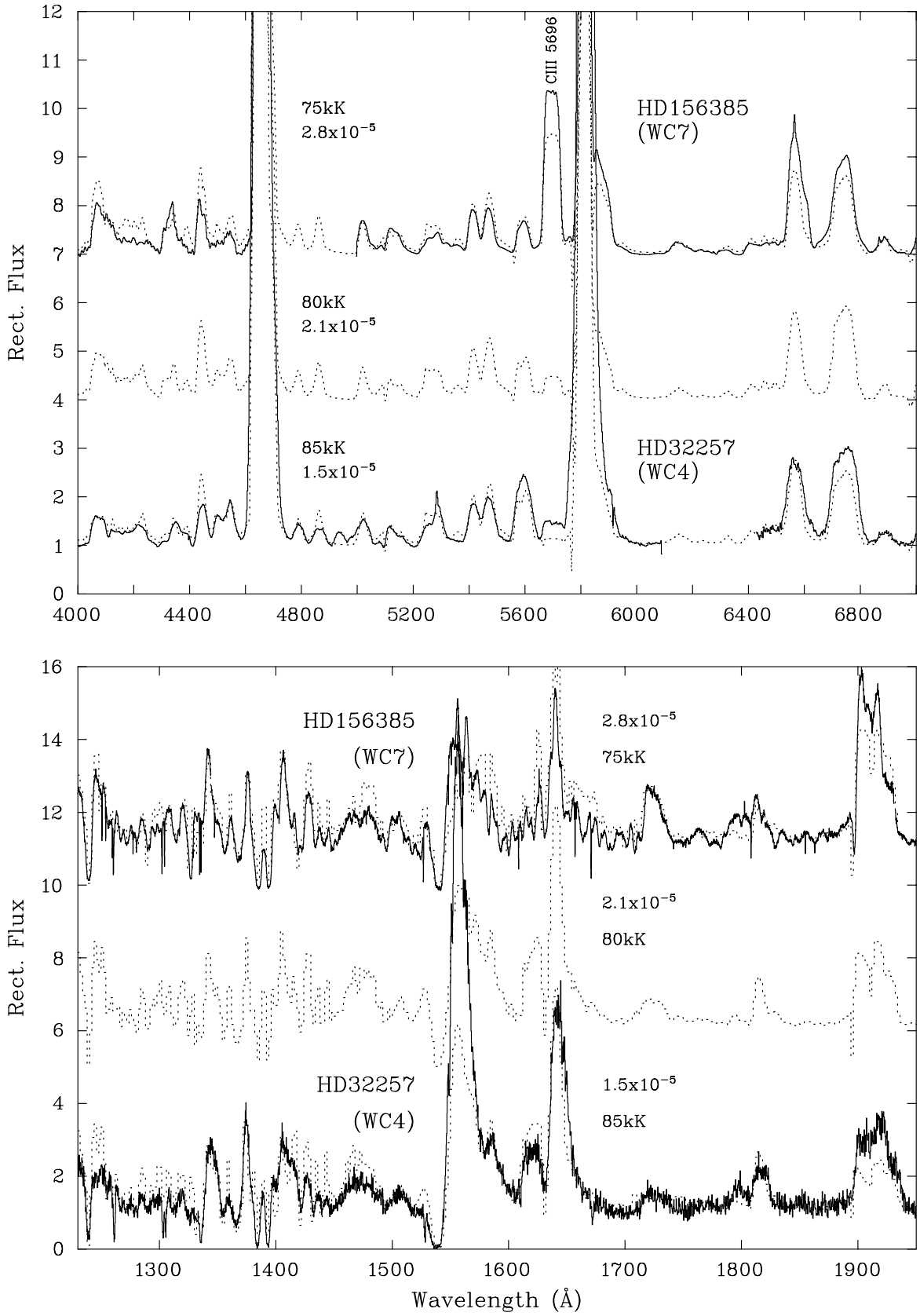

Fig. 12. Rectified optical (upper panel) and UV (lower panel) spectroscopy of HD156385 = WR90 (WC7, Galactic) and HD 32257 = Br 8 (WC4, LMC), together with synthetic spectra from a series of three models, with $\log(L/L_{\odot}) = 5.49$, $v_{\infty} = 2300$ km s^{-1}, C/He = 0.35 and O/He = 0.06, except that (bottom to top) the temperature:mass-loss rate is 75kK:2.8×10^{-5} $M_{\odot}$ yr^{-1}, 80kK:2.1×10^{-5} $M_{\odot}$ yr^{-1}, and 85kK:1.5×10^{-5} $M_{\odot}$ yr^{-1}, respectively. Remarkably, these small changes in stellar parameters closely match the optical and UV spectra of these WC4 and WC7 stars, with C III λ5696 most sensitive to small changes in physical parameter (compare λ5696 with λ6740 in the upper panel).

results in a slightly larger mass (Heger & Langer 1996). These calculations are presented in Table 7, together with masses derived from Langer (1989). Note that the differences are much smaller than those reported previously due to the reduced mass-loss rates for WR stars once clumping is taken into account. We have confidence in our derived masses due to the close agreement between the mass of the WC8 component in γ Vel obtained here from a previous spectral analysis ($\sim$9 $M_\odot$) with that obtained from an orbital study of this binary system (9.5 $M_\odot$, De Marco et al. 2000).

Further, in order to estimate final masses we make the following assumptions:

- Lifetimes remaining prior to a supernova explosion can be adopted from recent evolutionary models. For example, HD 32125 (for which C/He = 0.18 by number) is predicted to end its life in 3.7×10^5 yr according to the 0.4 $Z_\odot$ tracks from Meynet et al. (1994) irrespective of its initial mass (in the range 60–120 $M_\odot$). Alternatively, Meynet & Maeder (2000) have presented evolutionary tracks for rotating (solar metallicity) massive stars – following their predictions at 40 $M_\odot$ a much lower remaining age is obtained – 0.9×10^5 yr. Since the dependence of metallicity and initial mass remains to be established for rotating models we consider both possibilities in Table 7;
- We adopt a mass (luminosity) dependent mass-loss rate for the remainder of the star's life, scaled according to Eq. (1) and using the Langer (1989) mass-luminosity relationship. For the above example with standard evolutionary tracks, the mass-loss rate is reduced from 1.6×10^{-5} to 0.7×10^{-5} $M_\odot$ yr^{-1} over the next 3.7×10^5 yr, ending its life with a mass of 11.1 $M_\odot$.

Consequently, we consider final, pre-SN masses of 11–19 $M_\odot$ for the entire LMC sample. Given the systematically less luminous Galactic stars, we determine correspondingly lower final masses of 7–14 $M_\odot$ for these stars.

In addition, we are able to estimate the total amount of carbon released by the star throughout its WC lifetime which we have calculated as follows. For each epoch we have determined the mass fraction of carbon, X_C, via quadratic or linear fits to predictions of X_C versus remaining lifetime from Meynet et al. (1994) or Meynet & Maeder (2000). The amount of carbon liberated is then simply the product of the age interval, age dependent mass-loss rate (see above) and carbon mass fraction. In the above example, HD 32125 is predicted to lose a total of 2.2 $M_\odot$ of carbon during its WC phase using figures from Meynet et al. (1994) or 0.6 $M_\odot$ from Meynet & Maeder (2000). Our six WC4 targets are predicted to provide the LMC interstellar medium with 5–20 $M_\odot$ of carbon over their WC lifetimes.

6.2. What masses for type Ic SN?

It is possible to determine lower limits to the CO masses of type Ic SN from modelling their light curves and fitting expanding models to their early spectra. For example, Iwamoto et al. (1998, 2000) present fits to three SN Ic's, revealing CO core masses in the range 2.1 $M_\odot$ (SN 1994I), 10 $M_\odot$ (SN 1997ef), 13.8 $M_\odot$ (SN 1998bw). Recently, Smartt et al. (2002) have discussed potential precursors to the type Ic SN 2002ap in M 74, which include a WC star. From an examination of pre-SN images of this galaxy (with an LMC like metallicity), they deduced an upper limit of $M_B = -6.3 \pm 0.5$ mag for the immediate pregenitor. The brightest of our six WC stars has $M_b = -5.3$ mag, which corresponds to $M_B = -5.8$ mag in the Johnson system. None of these stars would have been visible on pre-SN images, adding substance to a possible WC precursor to SN 2002ap.

The values presented above represent minimum values of the final progenitor mass, since an unknown fraction may have imploded to form a black hole or other compact object. Nevertheless, the CO ejecta mass of SN 1998bw fits in remarkably well with the predicted final masses of LMC WC stars determined here. Evolutionary predictions, plus model analyses, imply that He represents a non-negligible fraction of the final surface abundance of very massive stars. This is consistent with the initial He-free type-Ic classification for SN 1998bw, since subsequent observations did reveal the presence of He I 1.083 μm (Patat et al. 2001).

SN 1998bw was also remarkable in that it appeared to be co-incident with GRB 980425. This Gamma Ray Burst was relatively sub-luminous, and it has been argued by Woosley et al. (1999) that such outbursts are atypical for GRBs. Nevertheless, SN 1998bw/GRB 980425 most likely corresponds to the collapsed core of a very massive star at the end of its WC phase. Recent XMM-Newton observations of GRB 011211 by Reeves et al. (2002) provides further support for such an origin due to enriched Mg, Si, S, Ar, Ca and Ni in the X-ray afterglow.

The lower CO mass of SN 1997ef is consistent with that of a luminous WC stars in our Galaxy, such as HD 165763 (WR111, WC5) for which we obtain a final mass of 10–12 $M_\odot$. The exceptionally low CO mass of SN 1994I has no analogue amongst Galactic or LMC massive WC stars, unless most of the final CO mass imploded as a black hole/neutron star.

7. Conclusions

We have used far-UV, UV, optical and near-IR spectroscopy together with line blanketed model atmospheres to re-evaluate the stellar parameters of six LMC WC4 stars. We derive stellar luminosities which are a factor of $\sim$2 higher than previously established for these stars (Gräfener et al. 1998), and systematically higher than Galactic counterparts at known distance. Mass-loss rates are lower than previously determined due to the inclusion of clumping in our models. Several lines of evidence, in both WN and WC stars, strongly suggest that the winds of WR are strongly clumped.

We find that the LMC WC4 stars possess very similar surface abundances to Galactic WC5–8 stars, although their wind densities are systematically lower, by $\sim$0.2 dex. We propose that the lower heavy metal content of the LMC is responsible for their lower mass-loss rates via their (still unproven) radiatively driven winds. A metallicity dependence of $\sim Z^{0.5}$ would produce this weak effect, comparable to that predicted for O stars as a function of metallicity ($\dot{M} \propto Z^{0.5-0.7}$: Kudritzki & Puls 2000; Vink et al. 2001). This relatively minor difference

quantitatively explains their different subtype distribution (recall Fig. 12). Temperature appears to be a secondary criteria in distinguishing WC4–WC7 stars. Late-type WC stars, especially WC9, do appear to be rather different, with systematically lower stellar temperatures. Looking at the broader picture of the subtype distribution in other Local Group galaxies, other factors clearly come into play.

If metallicity were the sole factor which determined the wind strengths of WC stars, those galaxies with metallicities close to Galactic (e.g. M 33 and M 31) would have a large, late-type WC population, which is apparently not the case (Massey & Johnson 1998), unless these are all obscured in the visible by circumstellar dust. Recent evidence suggests that most (or all) WC9 stars are close binaries with time-dependent dust production from interactions between the winds of the WC and OB companion (e.g. Tuthill et al. 1999). Future quantitative studies of the properties of these and more distant WR stars will hopefully help address these issues. Regardless of these details, the identification of a heavy metallicity dependence of WR winds has a major impact on their relative contribution to the hard ionizing photons in young starburst galaxies (Smith et al. 2002).

The association between spectral type and wind density amongst LMC and Galactic WCE stars also has relevance to the long standing debate amongst [WC]-type central stars of Planetary Nebulae (CSPN). It has long been recognised that [WC] stars positively avoid WC5-7 spectral types, and either cluster around WC4/WO or WC8–10 (e.g. Fig. 2 in Acker et al. 1996; Crowther et al. 1998). A wind density origin for the differences between WC4–7 stars (rather than temperature) can therefore explain the observed clustering as due to reduced wind densities amongst [WC]-type CSPN relative to massive Galactic WC stars, without the need to infer rapid evolution, for instance. Clearly, one still would need to understand why [WC]-type CSPN possess weaker winds than their massive cousins, but the differences would not need to be great – a factor of ~2 would suffice.

Finally, we determine current masses of LMC and Galactic WC stars including the (minor) effect of wind darkening (Heger & Langer 1996). Based on remaining lifetimes from evolutionary predictions we estimate final pre-SN masses of 11–19 $M_{\odot}$ for LMC WC stars, and 7–14 $M_{\odot}$ for Galactic WC stars with known distances. These values are consistent with WC stars being the immediate precursors to luminous type-Ic supernova explosions, including SN 1998bw and SN 1997ef.

Acknowledgements. *FUSE* is operated for NASA by the Johns Hopkins University under NASA contract NAS5-32985. The NASA/ESA Hubble Space Telescope is operated by AURA under the NASA contract NAS5-26555. Financial support is acknowledged from the Royal Society (PAC) and the UCL Perren Fund (LD). JDH acknowledges support by NASA through grants 4450.01-92A, NAWG-3828, plus 5460.01-93A from the STScI. Part of this research was carried out during a visit by JDH to London, which was funded via the PPARC grant PPA/V/S/2000/00500. We are indebted to the members of the OPACITY project, IRON project, plus Bob Kurucz, for their continuing endeavours to calculate atomic data without which studies presented above would not be possible. We are grateful to Kenneth Brownsberger for allowing his Guaranteed *FUSE* Time to be used for the study of Wolf-Rayet stars, to Jason Tumlinson for the use of his IDL-based molecular hydrogen fitting tool, and to Goetz Gräfener for calculating a test model using the current version of his model atmosphere code. Finally, thanks to the referee, Agnes Acker, for valuable comments.

References

Acker, A., Gorny, S. K., & Cuisinier, F. 1996, A&A, 305, 944
Bartzakos, P., Moffat, A. F. J., & Niemela, V. S. 2001, MNRAS, 324, 33
Breysacher, J. 1981, A&AS, 43, 209
Breysacher, J., Azzopardi, M., & Testor, G. 1999, A&AS, 137, 117
Cardelli, J. A., Clayton, G. C., & Mathis, J. S. 1989, ApJ, 345, 245
Conti, P. S., & Massey, P. 1989, ApJ, 341, 113
Conti, P. S., Massey, P., & Vreux, J. M. 1990, ApJ, 354, 359
Crowther, P. A. 1999, Wolf-Rayet Phenomena in Massive Stars and Starburst Galaxies, Proc. IAU Symp. 193, ed. K. A. van der Hucht, G. Koenigsberger, & P. R. J. Eenens (Kluwer, Dordrecht), 116
Crowther, P. A. 2000, A&A, 356, 191
Crowther, P. A., De Marco, O., & Barlow, M. J. 1998, MNRAS, 296, 367
Crowther, P. A., Pasquali, A., De Marco, O., et al. 1999, A&A, 350, 1007
Crowther, P. A., Fullerton, A. W., Hillier, D. J., et al. 2000, ApJ, 538, L51
De Marco, O., Crowther, P. A., Schmutz, W., et al. 2000, A&A, 358, 187
Dessart, L., & Owocki, S. P. 2002a, A&A, 383, 1113
Dessart, L., & Owocki, S. P. 2002b, A&A, submitted
Dessart, L., Crowther, P. A., Hillier, D. J., et al. 2000, MNRAS, 315, 407
Dufour, R. J. 1984, in Structure and Evolution of the Magellanic Clouds., IAU Symp. 108, ed. S. van den Bergh, & K. S. de Boer (Kluwer, Dordrecht), 353
Garmany, C. D., & Stencel, R. E. 1992, A&AS, 94, 211
Gräfener, G. 1999, Ph.D. Thesis, University of Potsdam
Gräfener, G., Hamann, W.-R., Hillier, D. J., & Koesterke, L. 1998, A&A, 329, 190
Gräfener, G., Koesterke, L., & Hamann, W.-R. 2002, A&A, 387, 244
Hamann, W.-R., & Koesterke, L. 1998, A&A, 335, 1003
Harries, T. J., Hillier, D. J., & Howarth, I. D. 1998, MNRAS, 296, 1072
Heger, A., & Langer, N. 1996, A&A, 318, 421
Herald, J. E., Hillier, D. J., & Schulte-Ladbeck, R. E. 2001, ApJ, 548, 932
Hillier, D. J. 1989, ApJ, 347, 392
Hillier, D. J., & Miller, D. L. 1998, ApJ, 496, 407
Hillier, D. J., & Miller, D. L. 1999, ApJ, 519, 354
Howarth, I. D. 1983, MNRAS, 203, 301
Howarth, I. D., Murray, J., Mills, D., & Berry, D. S. 1998, SUN 50.21 (Rutherford Appleton Laboratory)
Hummer, D. G., Berrington, K. A., Eissner, W., et al. 1993, A&A, 279, 298
Iwamoto, K., et al. 1998, Nature, 395, 672
Iwamoto, K., Nakamura, T., Nomoto, K., et al. 2000, ApJ, 534, 660
Koesterke, L., & Hamann, W.-R. 1995, A&A, 299, 503
Kudritzki, R.-P., & Puls, P. 2000, ARA&A, 38, 613
Langer, N. 1989, A&A, 220, 135
Lee, M. G., Freedman, W. L., & Madore, B. F. 1993, ApJ, 417, 553
Lundstrom, I., & Stenholm, B. 1984, A&AS, 58, 163
Massey, P., & Johnson, O. 1998, ApJ, 505, 793

Meynet, G., & Maeder, A. 2000, A&A, 361, 101
Meynet, G., Maeder, A., Schaller, G., Schaerer, D., & Charbonnel, C. 1994, A&AS, 103, 97
Moos, H. W., Cash, W. C., Cowie, L. L., et al. 2000, ApJ, 538, L1
Morris, P. W., Brownsberger, K. R., Conti, P. S., Massey, P., & Vacca, W. D. 1993, ApJ, 412, 324
Nugis, T., & Lamers, H. J. G. L. M. 2000, A&A, 360, 227
Panagia, N., Gilmozzi, R., Macchetto, F., Adorf, H.-M., & Kirshner, R. P. 1991, ApJ, 380, L23
Patat, F., Cappellaro, E., Danziger, J., et al. 2001, ApJ, 555, 900
Puls, J., et al. 1996, A&A, 305, 171
Reeves, J. N., et al. 2002, Nature, 416, 512
Royer, P., Smartt, S. J., Manfroid, J., Vreux, J.-M. 2001, A&A, 366, L1
Sahnow, D. S., et al. 2000, ApJ, 538, L7
Schaerer, D., & Maeder, A. 1992, A&A, 263, 129
Schlegel, D., Finkbeiner, D., & Davis, M. 1998, ApJ, 500, 525
Schmutz, W. 1997, A&A, 321, 268
Schmutz, W., Leitherer, C., & Gruenwald, R. 1992, PASP, 104, 1164
Seaton, M. J. 1979, MNRAS, 187, 73
Seaton, M. J. 1987, J. Phys. B., 20, 6363
Seaton, M. J. 1995, The Opacity Project, vol. 1 (Institute of Physics Publishing, Bristol)
Shortridge, K., Meyerdierks, H., Currie, M., et al. 1999, SUN 86.17 (Rutherford Appleton Laboratory)
Smartt, S. J., Crowther, P. A., Dufton, P. L., et al. 2001, MNRAS, 325, 257
Smartt, S. J., Vreeswijk, P. M., Ramirez-Ruiz, E., et al. 2002, ApJ, 572, L147
Smith, L. F., Shara, M. M., & Moffat, A. F. J. 1990, ApJ, 348, 471
Smith, L. F., & Maeder, A. 1991, A&A, 241, 77
Smith, L. J., Norris, R. P. F., & Crowther, P. A. 2002, MNRAS, in press [astro-ph/0207554]
Torres, A. V., Conti, P. S., & Massey, P. 1986, ApJ, 300, 379
Torres, A. V., & Massey, P. 1987, ApJS, 65, 459
Torres-Dodgen, A. V., & Massey, P. 1988, AJ, 96, 1076
Tumlinson, J., Shull, J. M., Rachford, B. L., et al. 2002, ApJ, 566, 857
Tuthill, P., Monnier, J., & Danchi, W. 1999, Nature, 398, 487
van der Hucht, K. A. 2001, New Astron. Rev., 45, 135
Vink, J. S., de Koter, A., & Lamers, H. J. G. L. M. 2001, A&A, 369, 574
Walborn, N. R., Howarth, I. D., Lennon, D. J., et al. 2002a, AJ, 123, 2754
Walborn, N. R., Fullerton, A. W., Crowther, P. A., et al. 2002b, ApJS, 141, 443
Woosley, S. E., Eastman, R. G., & Schmidt, B. P. 1999, ApJ, 516, 788